Discover Applied Sciences

RESEARCH Open Access

Investigation of graphene addition to a mixture of biodiesel and tire pyrolysis oil: impact on engine performance and emissions characteristics

Sadashiva Prabhu S[1], Kapilan Natesan[2], Shivaprakash Y M[1], Norkhairunnisa Mazlan[3] and Gurumurthy B M[1*]

*Correspondence:
Gurumurthy B M
gurumurthy.bm@manipal.edu
[1]Department of Mechanical and Industrial Engineering, Manipal Institute of Technology, Manipal Academy of Higher Education, Manipal 576104, Karnataka, India
[2]NITTE (Deemed to be University), Nitte Meenakshi Institute of Technology, Department of Mechanical Engineering, Bengaluru 560064, India
[3]Department of Aerospace Engineering, Faculty of Engineering, Universiti Putra Malaysia (UPM), Serdang 43400, Selangor, Malaysia

Abstract

In many countries, the disposal of waste tires poses a serious environmental threat, leading to air, soil, and water pollution. This problem can be effectively mitigated by converting waste tires into fuel through pyrolysis. In this study, two major innovations were introduced: the incorporation of tyre pyrolysis oil (TPO) as a blend to biodiesel to enhance its volatility and combustion characteristics, and the use of graphene nanoplatelets as an additive to further improve combustion efficiency and reduce exhaust emissions owing to their superior thermophysical properties. The engine tests conducted with a blend of 80% Karanja biodiesel and 20% TPO(B80T20) at constant speed and varying loads demonstrated that the combined addition of TPO and graphene significantly improved brake thermal efficiency and reduced harmful emissions. The optimum graphene concentration of 75 mg/L yielded a 6.2% increase in brake thermal efficiency, an 8.94% rise in exhaust gas temperature, an 18.75% reduction in CO, 25% reduction in HC, an 8.16% increase in nitrogen oxides, and a 10.16% decrease in smoke levels compared to B80T20 at full load. Furthermore, regression analysis was performed to correlate engine performance and emission characteristics, and a cost analysis with graphene addition was conducted to assess the economic viability of the proposed approach.

Highlights

- Studies on enhancement of biodiesel fuelled engine and reduction in emission characteristics.
- Experimental investigation on effect of graphene addition to the mixture KOB and TPO comprising brake thermal efficiency and emission characteristics.
- Regression analysis of BTE and emission parameters with different dosages under varying engine load conditions.
- Evaluation of optimum dosage of graphene based on thermal performance and emission analysis.

Keywords KOB, Tyre pyrolysis oil, Graphene, Engine, FTIR

1 Introduction

Many countries around the world are large energy consumers. Energy seems to be the backbone of any economy, and oil was a key energy source for industry in the 19th century [1]. Population growth and industrialization resulted in intensifying fears about energy scarcity, climate change, and the persistent growth in energy requirements. It is advisable to take various measures to increase energy efficiency and demand-side management, especially in the transport sector. Due to climate change and energy security concerns, strong attention has been given to finding a substitute for the rising energy demand [2]. Alternatively, it is worthwhile to strengthen renewable biofuels and increase their usage. Conventional diesel engines are an area of interest which used most heavy-duty purposes, and numerous studies have been conducted in recent years to understand improvements in efficiency and reductions in emission levels, aiming to reduce running costs. Due to the increase in demand and price, and to meet emission regulations, blended biodiesel is an alternative to conventional fuels [3]. Renewable biofuels, replacing diesel, have started to take a role in global energy policy, and countries like Brazil have used them since 1929 [4]. Moreover, liquid biofuels may offer a quick remedy to the problem of fuel supply insecurity for transportation, despite the fact that the industry for liquid biofuel production is not yet fully developed. This situation is linked to several factors, including the nature of the raw materials utilized, the specific methods employed in biodiesel production, and the proportion of blending or mixing with other fuels and additives [5]. Biofuels are generally eco-friendly in terms of being biodegradable, sulfur-free, and non-toxic, compared to other traditional fuel sources. Global demand for biofuels is expected to increase by 41 to 53 billion liters, or 28%, from 2021 to 2026 [6]. Some of the advantages, limitations, economics, comparative analysis, and results of various researchers are found in the literature [7].

Production of biodiesel from wastes obtained from agriculture, industrial wastes, municipal wastes, waste cooking oil, waste animal fat, etc. Is important for sustainability and it can be used to achieve renewable and sustainable goals. The biofuel policy and green shipping encourages the extraction of biodiesel from non-edible oils [8]. Various methods of production of biodiesel and feedstocks are emphasized in the literature [9, 10]. Due to the high production costs of a few biodiesel, novel environmentally friendly biofuel with newer technologies are being developed [11]. With regard to usage point of view, there are some challenges to face when using biodiesel in engines, such as oxidation stability and spray atomization, as these properties are affected by the viscosity, density, and surface tension of biodiesel. Biodiesel's oxidation stability can be improved by using antioxidants [12]. Performance of the biodiesel-operated diesel engine showed improvement for high injection pressure due to better atomized spray [13, 14]. Further, ignition delay of biodiesel is shorter than that of diesel [15]. In order to reduce its higher viscosity, improve its atomization, vaporization, and fuel-air mixing few researchers followed preheating method, indicated that preheated crude palm oil (CPO) led to lower exhaust emissions, including reduced levels of CO, HC, and PM when compared to OD and emulsified fuels made with CPO [16]. Heterogeneous catalysts are preferred, as they are especially good at generating high amounts of FFA (free fatty acid) in the feedstock [17]. WCO biodiesel production options are low-cost and have well-developed collection and processing infrastructure [6]. So, cost, usage, need and issues to be thoroughly assessed before the use the biodiesel.

1.1 Significance of blending of biodiesel, associated issues and remedies

Different studies related to combustion, emission properties, and trace metal concentrations in particulates from biodiesel exhausts have been found in the literature [18–20]. In summary, the addition of biodiesel to the test fuels increased the brake-specific fuel consumption (BSFC), while the brake thermal efficiency (BTE) of biodiesel blends was marginally lower than that of mineral diesel. Increasing the percentage of biodiesel blends without engine modification is a matter of interest. Likewise, studies have been conducted on B10, B20, and B30 fuels by several authors, who suggested that up to a 10% biodiesel blend engine modification is not required. According to them, B10 is the optimum biodiesel blend for BTE [21]. Meanwhile, few researchers have focused their attention on ternary blends. The analysis done by Sudalaiyandi et al. [22] indicated that ternary blend 1 (5% biodiesel, 5% biodiesel rubber, and 90% diesel) and blend 2 (10% biodiesel linseed, 10% biodiesel rubber, and 80% diesel) had better performance. It is reported that ternary blends produce fewer NO_2 and CO emissions compared to baseline diesel. This hints towards blending biodiesel and decrease in emissions.

Efforts are essential to increase the blend percentage. In that context, the preheating process [16] decreases the viscosity of CPO to match that of ordinary diesel, thereby enhancing the spray and atomization qualities of the fuel and resulting in more complete combustion. It is suggested that this could even be a method to increase BTE and reduce emissions. As the preheating process requires additional energy, the authors realized that suitable secondary blend may increase BTE and reduce emissions by enhancing biodiesel's burning characteristics. To increase the blend percentage and also to overcome the above-stated problem of viscosity and to enhance burning characteristics, it is required to use a secondary blend. In that direction researchers have also focussed their attention on extraction of oil from waste tyres (tyre pyrolysis oil) as it is available in abundant quantities. It is a sustainable source that can be used either as a primary blend or a secondary blend which may reduce operational cost and may reduce problems associated with primary blend. Furthermore, limited studies were found on the blending of TPO with various biodiesel in excess quantities. The benefits of adding both TPO to KOB are explained in the following sections.

1.2 Blending TPO with KOB

Biodiesel offers excellent combustion characteristics due to its high oxygen content but can have higher cost and lower energy content than conventional diesel. Mixing biodiesels will benefit in cost and properties perspectives. Few authors have identified that mixing biodiesel like waste cooking oil biodiese (50%) and pongamia oil biodiesel (50%), reduces production costs and processing time. However, biodiesel has higher viscosity and lower volatility and needs additive to overcome these issues, and low-cost volatile fuel can be used as its partial substitute. In that context, TPO can be a suitable fuel that could be blended with biodiesel, and it mixes with biodiesel. Combustion of TPO is similar to diesel when tested in a common rail, modern turbocharged, and inter-cooled engine with EGR [23]. More benefits of using TPO in engines are highlighted by Murugan et al. [24]. Among them, the BTE was found to increase with an increased blend percentage from 10 to 50% and no blocking of the injector or any seizing of the engine was observed during testing.

An experimental study of hybrid fuel blends (TP10KB20, TP20KB10) and equivalent source blends (TPO30, KBD30, and diesel) is conducted on a single-cylinder CI engine. The performance and combustion of TP10KB20 and TP20KB10 have been demonstrated to be superior to those of all other single blends and diesel fuels [25]. Few studies have shown that the engine is able to run on blends of TPO and hemp oil at different loads, exhibiting similar performance to diesel [26]. However, the biodiesel content was limited to 10%. It was interesting to observe how adding 100 ppm of cerium oxide NPs to a diesel - TPO mixture increased the maximum cylinder pressure at various engine loads [27]. So, the addition of NPs more advantageous in several aspects when biodiesels are used in engines. More details are explained following section.

1.3 Significance of adding NPs and the beneficial effect of graphene

To enhance efficiency, NPs can be integrated with biodiesel mixtures. In addition, the use of NPs additives enhances engine performance, improves heat transfer rates, optimizes fuel mixture balance, modifies thermophysical properties, and reduces exhaust emissions.

The addition of NPs, such as titanium oxide, significantly enhances engine performance and reduces emission levels [28]. Integrating hybrid Al_2O_3 and GO NPs with dimensions of 20–30 nm into a blend of 20% waste oil biodiesel and 80% diesel could serve as a viable fuel option for commercialization in CI engines without requiring any modifications to the engine [29]. A notable improvement has been observed in BTE for nanoparticle-enhanced disperse test fuels. The highest increase in BTE recorded was up to 24.7% when using a blend of Jatropha biodiesel (B20) with 50 ppm of Al_2O_3 NPs. A maximum reduction of 25% in BSFC was noted for a biodiesel blend with 150 ppm of TiO_2. Further, reductions up to 70.94% for HC, 80% for CO, and 30% for NO_x in a methyl ester of WCO(B10) when blended with 100 ppm of TiO_2, JB20 when mixed with 20 ppm of Al_2O_3, and WCO B10 combined with 30 ppm of Al_2O_3 and 30 ppm of CeO_2, respectively [30]. Copper oxide, a type of transition metal oxide, helps facilitate heat transfer from the engine to the exhaust, consequently reducing NO_x emissions. Therefore, CuO NPs are considered to have significant potential as an additive for diesel engines [31]. Higher combustion temperatures were linked to an increase in NO_x emissions, but a notable decrease in CO and particulate matter emissions, according to an emission study that utilized CNTs.

Although they were slightly less successful than CNTs, ZnO and Al_2O_3 also improved fuel atomization and combustion. This study demonstrates that biodiesel blends made with NPs, particularly when CNTs are added, can significantly improve engine performance and reduce emissions from incomplete combustion, but managing NO by carbon-based NPs additions in biodiesel blends will be essential to its widespread use [32]. This envisages an insight to carbon based nano into carbon-based NPs additions in biodiesel blends particle additions in biodiesel blend.

In that case, problems such as poor fuel properties and increased NOx emissions have hindered its widespread use. To overcome these limitations, a few authors studied the effects of antioxidants derived from leaf extract (NLA), eucalyptus leaf extract (ELA), and pongamia leaf extract (PLA) [33]. To enhance the combustion and emission properties of DB10 fuel, MWCNT was added. With MWCNT, fuel consumption dropped and thermal efficiency increased. MWCNT decreased ignition latency by raising cylinder

pressure and heat release. MWCNT mixes significantly reduced emissions of CO, HC, and smoke. With MWCNT, NO_x emissions rose, suggesting a trade-off in combustion behaviour [34].

Limited studies were found in the literature on the performance and emission characteristics of biodiesel when used beyond 20% along with additives. Furthermore, the behavior and contribution of NPs to effective burning, particularly when biodiesel is in excess, need to be understood and are not discussed extensively in the literature.

Graphene (GR), due to its basic structure, has a large area-to-thickness ratio, which may improve its evaporation and burning characteristics. As observed, the evaporation of the tiny fuel droplets from the fine spray that occurs in the combustion chamber is broken by the fuel droplet. The viscosity, intermolecular bonding, and surface tension of the biodiesel are higher. The use of GR may accelerate evaporation by reducing intermolecular interaction and breaking the fuel droplets into microscopic particles.

As GR possesses high thermal conductivity, it can be utilized in heat transfer applications as nanofluids [35], and its addition enhances the engine's BTE compared to biodiesel blends [36]. Because GR has special thermal and physical properties, researchers are interested in applying GR and its derivatives to a wide range of applications, including the combustion of biofuels [37]. It is also reported that GR exhibits superior characteristics compared to other metal oxide NPs in terms of limiting micro explosions during fuel combustion [38]. Also, it burns with biodiesel and does not cause any kind of pollutants like metal oxide NPs. Further, GR's excellent thermal conductivity, large surface area, and electrical conductivity influence the ignition process. Furthermore, the behavior of GR in the presence of a secondary blend, such as TPO, remains unknown. The variation in performance and emission levels with an increase in GR dosage for various biodiesel combinations is a matter of interest for optimum usage.

Adding GR to biodiesel blends improves the physical and chemical properties of the fuel through several mechanisms. GR's high surface area and catalytic activity promote the breakdown of larger fuel molecules into smaller, more reactive species during combustion, enhancing fuel oxidation and energy release. Its exceptional thermal conductivity facilitates efficient heat transfer, enhancing combustion stability and reducing ignition delay. GR also interacts with the fuel at a molecular level, altering its viscosity and density to optimize spray characteristics and improve air-fuel mixing in the combustion chamber. These combined effects enhance fuel combustion efficiency, reduce emissions, and optimize engine performance. In some cases, this type of additive has contributed to a notable improvement in engine performance for 20% blended fuel [39].

Considering the above factors, we have chosen B80T20 (80% KOB + 20% TPO) as the base fuel to investigate the benefits of adding GR. Further, TPO has a higher calorific value than KOB and their blends (Table 1). Therefore, it is used as a blend for KOB in the

Table 1 Engine details

Engine	Four-stroke, single-cylinder
Make and model	Kirloskar; model TV1
Engine bore (mm)	87.5
Engine stroke (mm)	110
Compression ratio	17.5: 1
Maximum brake power (kW)	5.2 at 1500 rpm
Injection timing	23°bTDC
Injection pressure (bar)	200

present case, with KOB in excess (80%) and no diesel content. The study aims to assess the impact of adding GR on engine performance, soot characteristics, and emission patterns, thereby addressing environmental issues associated with conventional fuels while offering a high-performance and sustainable alternative fuel choice by investigating the synergistic effects of graphene.

According to the literature survey, it was observed that Karanja oil biodiesel (KOB) exhibits relatively higher viscosity and lower volatility, which limits its combustion performance. To overcome these drawbacks, there is a need for novel, low-cost additives. In this study, two key innovations were introduced: the incorporation of TPO, a fuel with higher volatility that enhances the recyclability of waste tires for sustainable energy development and the addition of GR, known for their exceptional thermophysical properties, to improve combustion and emission characteristics. The optimal GR dosage in the KOB–TPO blend was determined experimentally to achieve the best performance outcomes.

The key novelty of this study lies in the combined utilization of TPO and GR with biodiesel, a hybrid additive strategy that has not been widely explored, to simultaneously overcome viscosity challenges, enhance volatility, and improve combustion performance. This synergistic blend is investigating its impact on engine performance and emission behavior, offering a new pathway for optimizing biodiesel-based fuels. So, the present study involves dual innovation: (1) the synergistic use of biodiesel and TPO, both derived from renewable or waste sources, and (2) the integration of GR to improve fuel characteristics. The engine tests with the above combination of fuel are proposed. Based on successful engine experiments, it is proposed to investigate the effects of TPO addition to biodiesel and the role of GR in modifying fuel behaviour for improved performance and emission characteristics. Furthermore, this work aims to optimize the GR concentration and analyse its impact on engine performance and emissions under various engine loads. The outcomes contribute to the development of high-efficiency, low-emission alternative fuels through the combined use of waste-derived fuel and advanced nanomaterial.

Prediction and optimization go in line with experimental investigation. The study's overall findings demonstrate the potential of tree-based ensemble learning, and extra trees in particular, as a lightweight, accurate and reliable tool for real-time emission prediction in low-carbon dual-fuel systems [40]. It is reported that the meta-regression found a significant positive association between increasing ratios of biodiesels and decreasing torque, engine power, CO and CO2 emissions, and increasing fuel consumption and NO emissions in terms of linear equations [41].

Response Surface Methodology is a technique to optimize input variables for various engine-related parameters, thereby limiting the number of experiments. The full factorial design (FFD) provides every possible combination of all factor levels, offering a comprehensive understanding of the process. FFD capacity to examine how several elements interact to affect the result is one of the main advantages. All two-way and higher-order interactions can be detected using a full factorial design without being confused with other effects. Regression analysis is typically performed on parametric responses with respect to variables. The regression equation, which is based on coded variables, will provide valuable information. In the present analysis, the BTE and other emission levels

have been studied with respect to dosage and load conditions. Experimental and RSM values are to be compared, and the error rate needs to be verified.

2 Experimental setup and procedure

2.1 Materials and methodology

In this work, KOB was used as a biodiesel and primary fuel and TPO was used as the secondary fuel. The fuel mixture was obtained by mixing 80% KOB and 20% TPO (Volume basis). The KO and TPO were procured from Bangalore, India. The GR concentrations, 50, 75, and 100 mg/L, were considered and added to the fuel mixture and subjected to ultrasonication to prepare a homogenous fuel mixture.

KO is an inexpensive, non-edible resource with considerable potential for biodiesel production. Due to its high acid value, a two-step transesterification process was selected for biodiesel synthesis. The oil-to-methanol molar ratio was determined to be 1:6. Sulfuric acid and potassium hydroxide were selected as catalysts for the first and second phases of the transesterification process, respectively. The temperature and duration for each transesterification step are set at 60 °C and 90 min, respectively. The TPO was sourced from the Peenya Industrial Area in Bangalore, India.

KOB, KOB + 20%TPO(B80T20), and KOB + 20%TPO(B80T20) with various concentrations of GR were prepared and addition of GR to the fuel mixture exhibited slight variation in appearance [42]. The GR quantities of 50, 75, and 100 mg were mixed with 1 L of B80T20 and sonicated for 60 min to obtain a homogeneous mixture. The properties of diesel, TPO, B80T20, and B80T20 with different GR concentrations have been determined according to ASTM standards. The engine tests were conducted with B80T20 as fuel to get baseline data. Then, the engine tests were conducted with B80T20 fuel mixture containing different dosages of GR. The open-burning tests were conducted with the fuel mixture, and the burnt materials were subjected to FTIR, SEM, and XRD analysis.

2.2 Experimental procedure

A performance test was conducted in an engine experimental setup, as shown in Fig. 1a and b. A diesel engine used for agriculture applications, was modified to conduct the experiments. The engine is a direct injection, water-cooled, and naturally aspirated type. The technical specification details are given in Table 2. Engine test setup is equipped with an airbox, manometer, fuel tank, fuel measuring unit, temperature sensors, transmitter, load measuring devices and process indicator. The measuring instruments were calibrated. The gas analyzer and smoke meters were used to collect the emission details; their specifications are provided in Table 3. Eddy current dynamometer was used to vary the engine load, as the load has a significant impact on both thermal performance and engine emissions [43]. Tests were conducted at steady state, and at the engine speed of 1500 rpm and the engine load was varied to full load from no load condition. The engine tests were conducted with all necessary safety precautions.

To establish a baseline data for diesel performance, experiments have been carried out using B80T20 fuel mixture at 1500 rpm. A leak test and purging were done prior to the emissions test, and a gas analyzer probe was kept in the exhaust stream. While changing fuel, previous fuel was drained out, and new fuel was made to circulate in the fuel supply

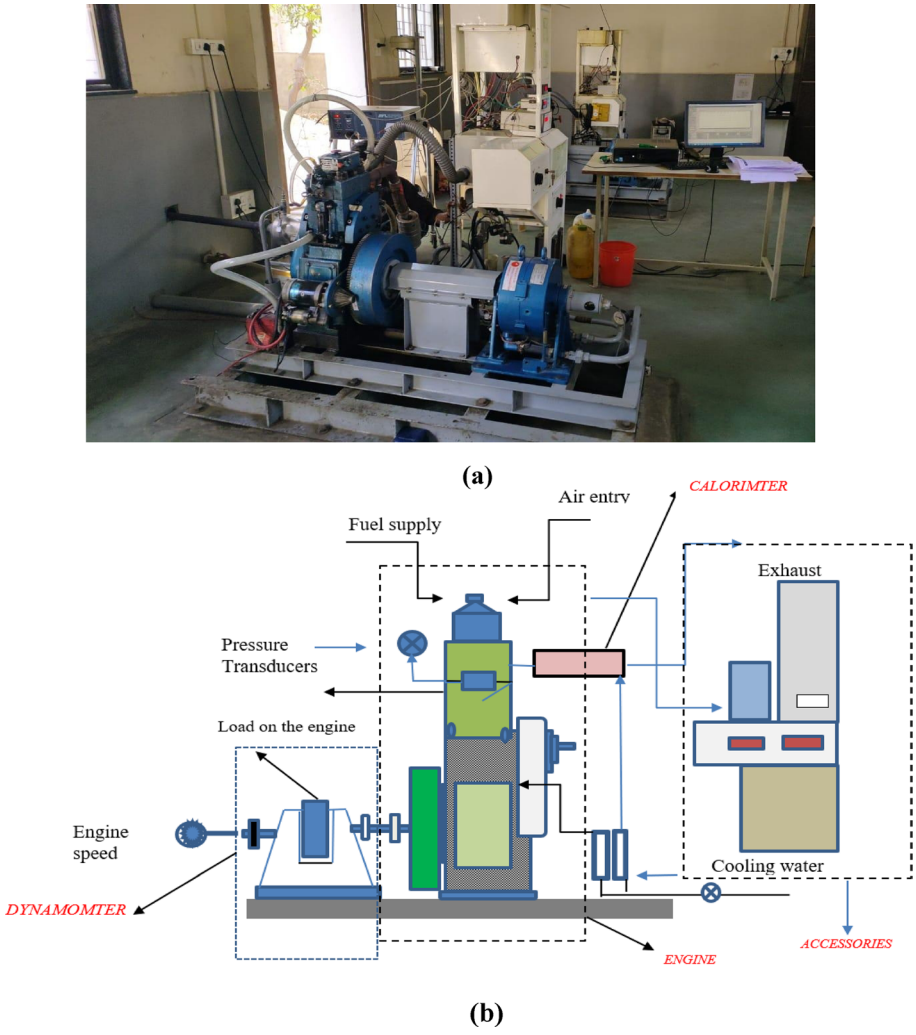

Fig. 1 **a**) Experimental setup **b**) Schematic diagram of engine setup

Table 2 Specification of engine exhaust gas analyzer and smoke meter

Make and model	**AVL DIGAS 444 *N***		
Exhaust gas species	Range	Accuracy	Uncertainty
CO (% vol)	0–15	−0.01 to + 0.01	±0.35
HC (ppm)	0 to 2×10^4	−10 to + 10	
NO_x (ppm)	0 to 5×10^3	−50 to + 50	
Smoke meter			
Make and model	AVL; 437 C		
Range (%)	0–100%	0.01 to + 0.01	

Table 3 Properties of fuels used

Sl.no	**Property**	**B80T20**	**B80T20G50**	**B80T20G75**	**B80T20G100**	**Diesel**	**TPO**
1	Flash Point (° C)	142	140	139	138	68	68
2	Density (kg/m^3)	872	874	875	877	841	924
3	Viscosity 40 ° C (mm^2s^{-1})	4.8	4.83	4.86	4.88	2.7	2.69
4	Calorific Value (MJ/kg)	37.1	37.3	37.4	37.6	42.9	43.225

system. To ensure the system with new fuel, 100 ml of fuel was collected, and after a 15-minute runtime of the engine, readings were taken thereafter.

Baseline data was obtained under steady-state conditions using B80T20 as the fuel. In the baseline study, the engine was run on B80T20, and its operating parameters, such as compression ratio, injection pressure, and injection timing, remained unchanged. The B80T20 was drained from the fuel supply system and fuel injector was then removed to drain the fuel mixture from the fuel line and from the fuel filter. After this, fuel injector was refitted, and the engine was made to run on B80T20G50 and then run again for 15 min to reach steady state. Similar procedure was followed for the B80T20G75 and B80T20G100 fuel mixture.

3 Results and discussion

3.1 Evaluation of properties of biodiesel and its blends

Two-step transesterification process used in this work results in biodiesel yield of 90%. Gas chromatography analysis was done at Bangalore Test House, Bangalore, India and the results showed that KOB contains various acids, including stearic, palmitic, oleic, behenic, linoleic, and arachidonic acids. GR nanoplatelets were added to fuel B80T20 and subejcted to ultrasonication to prepare a homogenous mixture and important fuel properties were determined as per ASTM procedures, and average values of three trails were considered for comparison. The properties of the B80T20, B80T20G50, B80T20G75, and B80T20G100, diesel and TPO, were determined and tabulated in Table 1. As observed, the flashpoint of the B80T20 decreases with the addition of GP due to better heat transfer. Increase in calorific value was observed with GR addition and this is because, GR is a carbon-rich nanomaterial with a high heating value, as its pure carbon structure and strong carbon–carbon bonds. GR contributes additional chemical energy during combustion, thereby increasing the overall calorific value of the fuel blend. However, there is a slight increase in density due to high carbon content and substantial mass per unit volume and also increase in viscosity due to interfere with the smooth flow of fuel molecules.

3.2 Variation of properties of biodiesel by adding TPO and graphene-blending characteristics

Figure 2a shows the FTIR analysis of KOB. The peaks between 2920.68 cm $^{-1}$ and 2860.8 cm^{-1} and 1350 cm^{-1} to 1480 cm^{-1} correspond to the C-H stretch of alkanes. The major absorption band corresponding to 1741 cm^{-1} indicates the presence of esters, which 1765–1735 cm^{-1} corresponds to C = O stretch.

Analysing the FTIR spectra of TPO as shown in Fig. 2b, the peaks at 2913.25 and 2853.476 cm^{-1} identified as C = C stretching and C-H stretching, respectively, represent the Alkanes group. Additionally, the FTIR of GR show some peaks at 2150 cm^{-1} and 3550–3650 cm^{-1} strong peaks (Fig. 2c). Figure 2d illustrates the FTIR comparison of KOB, B80T20, and B80T20 G100. A minor change in % transmittance is noted, but no new bonds are detected. Figure 2d represents the superimposed FTIR patterns of KOB, KOB + TPO, and KOB + TPO + GR. There is little variation in the pattern, indicating that adding TPO and GR does not alter the basic chemical nature.

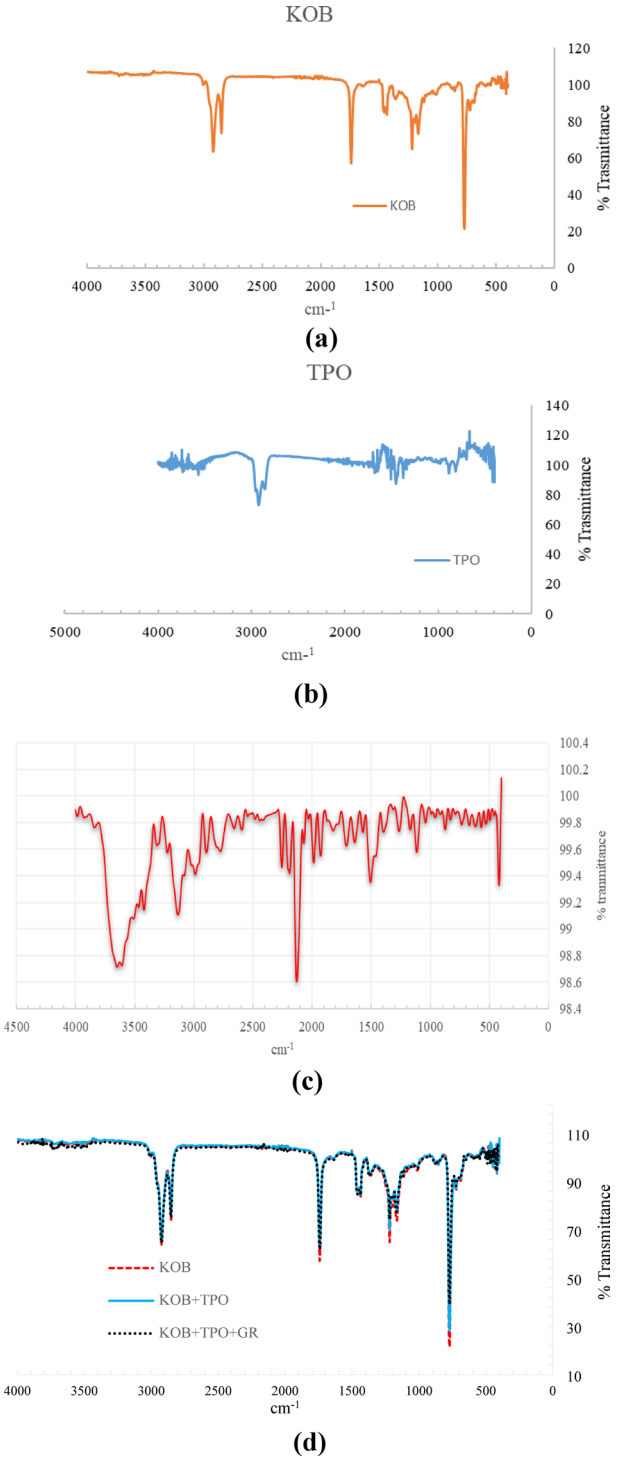

Fig. 2 The FTIR results of **a**) KOB, **b**) TPO, **c**) GR **d**) B80T20G100 when tested in initial stages

3.2.1 Properties of graphene through SEM/XRD

Structural characteristics of GR were examined via SEM, as shown in Fig. 3, demonstrating its two-dimensional(2D) sheet-like form. The XRD pattern of GR resembles that of graphite, as GR is inherently similar. (Fig. 4).

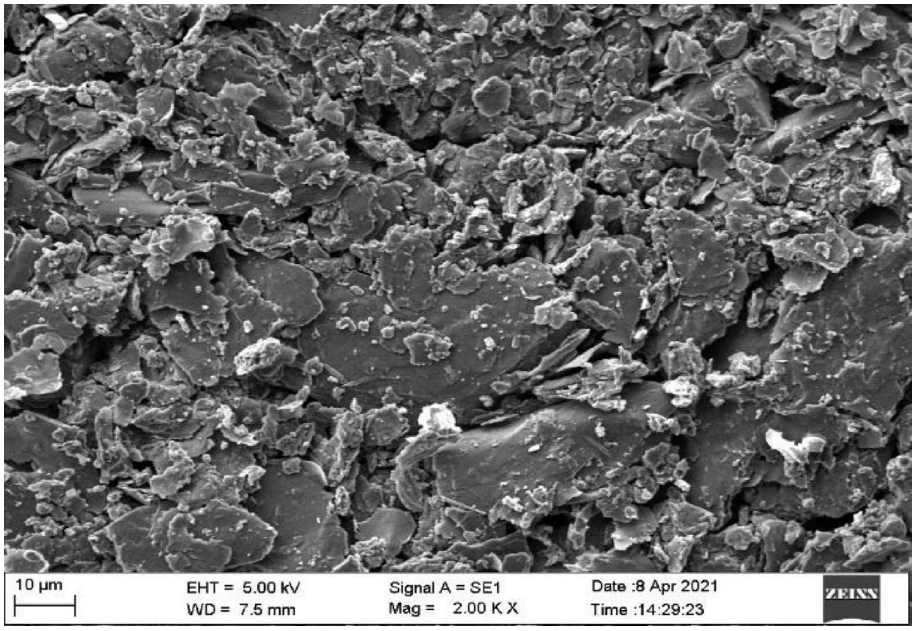

Fig. 3 SEM image of the GR

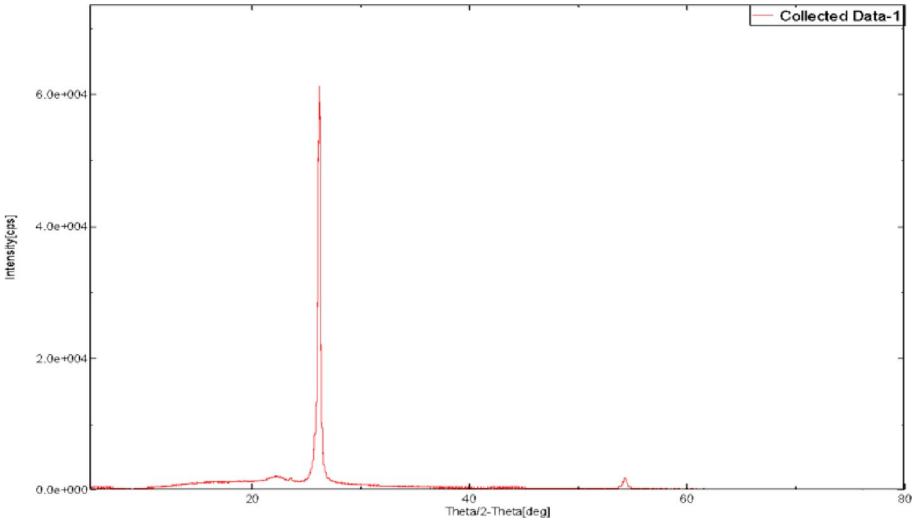

Fig. 4 XRD of GR

3.3 Engine performance studies

Without many modifications to the fuel injection systems, engine tests were carried out. The engine performance is discussed in subsequent sections. The BTE was determined by measuring brake power and the mass of fuel consumed. The BTE is the ratio of brake power to energy supplied by the fuel which is obtained by multiplying the mass of fuel consumed and calorific value. All the parametric studies done on performance and emission characteristics are presented in Fig. 5(a-f) and discussed in the next sections.

3.4 Thermal efficiency

Effect of GR on BTE for various load conditions is depicted in Fig. 5a and it shows that the BTE of B80T20 is lower than other fuel mixture and this is due to higher viscosity

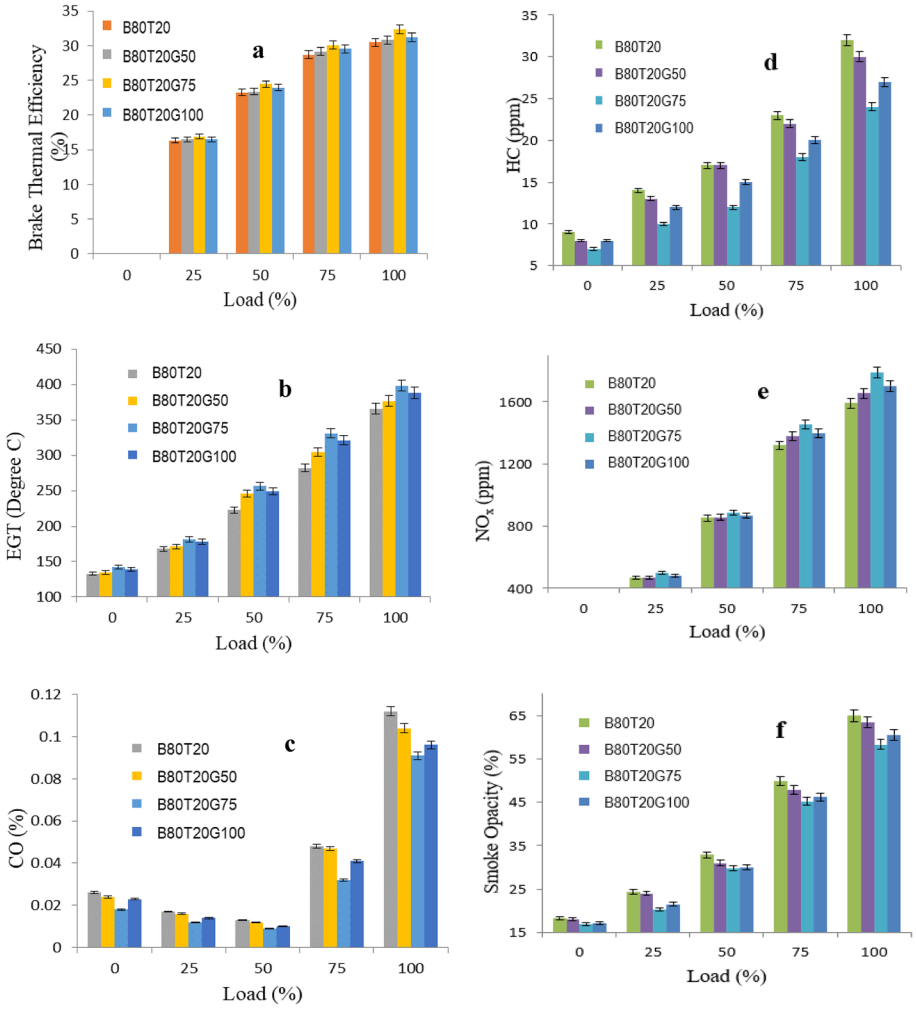

Fig. 5 Variation of **a**) BTE, **b**) EGT, **c**) CO, **d**) HC, **e**) NO_x **f**) Smoke opacity vs. load

of this fuel mixture which causes higher ignition delay, resulting in B80T20 having a lower pre-combustion phase and a higher diffusive phase. Addition of GR to B80T20 helps break down the biodiesel droplets into smaller droplets, thereby accelerating the fuel's evaporation [44]. However, increasing the addition of GR affects the BTE, so it must be optimized. For cases B80T20G75 and B80T20G100, a higher BTE is observed even at higher loads. This result aligns with the findings of other researchers [45]. The B80T20G50 finds lower BTE in comparison to B80T20G75 and B80T20G100, as it finds lower concentrations of GR. The B80T20G75 results in a 6.2% higher BTE than the B80T20 at full load, indicating that an increased concentration of GR beyond 75 mg/L adversely affects BTE.

Few studies in the literature show an increment in efficiency up to 18.93% with the addition of 75 mg/L GR for OCB20 (diesel-80% blended with oleander and croton biodiesel-20% 20% (OCB20) [46]. From the similar studies done by Bayindirli et al. [47] shown increment of 17.97% for cottonseed oil methyl ester. In our study, BTE is comparatively lower as B80T20 is used instead of diesel.

The optimum GR addition of 75 mg/L results in higher BTE due to the shorter ignition delay created by the GR. Also, the high calorific value of the graphene-emulsified

fuel leads to high combustion pressure and higher BTE. On the contrary, the higher GR dosage of B80T20G100 affects the spray formation of the fuel mixture, which affects the combustion pressure and, in turn, reduces the BTE of the engine [48]. So, optimization of graphene dosage is essential.

3.5 Temperature of exhaust gas

The addition of GR leads to an increase in exhaust gas temperature, as the carbon content in GR contributes energy and enhances combustion [49, 50]. Furthermore, it is also reported that the temperature of the exhaust gas increases due to an increase in brake mean effective pressure [51]. Figure 5b depicts the effect of the dosage of GR on exhaust gas temperature with varying load conditions. The EGT of B80T20G75 is higher than the B80T20G50 and B80T20G100 for increased load conditions. This trend is caused by poor atomization and spray resulting from ted due to lower dosages of GR, as observed even in the case of Bidir et al. [52]. The B80T20G75 results in an 8.9% higher EGT value than B80T20. A higher dosage of GR (G100) leads to agglomeration, which affects spray and combustion, resulting in poor burning and lower EGT. The study suggests that an increase in EGT occurs due to an increase in GR dosage up to a certain limit, after which it decreases.

3.6 CO emissions

Incomplete mixing of air and fuel leads to increased CO emissions due to rich zones of incomplete combustion. The CO also indicates poor combustion. However, the generation of CO in various fuel mixtures mainly results from the incomplete oxidation of the fuel, in contrast to traditional diesel. The CO variation of the B80T20 -fuelled engine with different GR dosages is represented in Fig. 5c. Further, the emission of CO increased for increased load conditions due to a reduction in the A/F ratio. The CI engine emits higher CO with B80T20 fuel at all loads than with other blends. The addition of GR to B80T20 enhances both premixed and diffusion combustion phases, resulting in lower CO levels. Higher heating values with the inclusion of GR generally lead to more energy output, resulting in less CO_2, as it is expected that CO converts into CO_2. Decrease in CO emission is attributed to the inclusion of GR in fuel mixture, which enhances the fuel's heating value and density, thereby leading to reduced CO emissions [52]. In the present case, the CO emission was significantly reduced by adding GR at a dosage of 75 mg/L, compared to other dosages. The premixed combustion improves due to a reduction in ignition delay caused by the addition of GR, resulting in lower CO levels compared to other dosages, as CO conversion to CO_2 is expected. The CO value is reduced by 18.75% for B80T20G75 when compared with that of B80T20. It has been found that incorporating 40 ppm of GO resulted in a peak decrease of 36.41% in CO emissions [53]. However, based on engine condition, injection timing, and injection pressure, CO values differ, even though excess biodiesel provides sufficient oxygen.

Higher thermal conductivity and larger surface area of GR enhance combustion by facilitating better fuel vaporization and improved heat transfer during B80T20 combustion, thereby reducing the CO level. The GR dosage of 75 ppm results in the lowest CO level, due to the better combustion achieved with the optimum GR dosage [48, 52]. From the similar studies done by Bayindirli et al. [47] shown decrement of 14.99% cottonseed oil methyl ester for(Gn-75) fuel cotton seed fuel.

3.7 HC emissions

Figure 5d depicts the variation of HC for B80T20 and different dosages of GR. HC emission is found to increase with the load. By observation, the HC emission is decreased when GR is added to biodiesel. In the case of B80T20, higher viscosity results in a higher diffusive combustion phase and a lower premixed combustion phase. GR breaks the biodiesel droplets into smaller ones, resulting in increased fuel and air mixing and enhanced fuel combustion, which leads to lower HC levels. Further, referring to Table 2, we observed that the heating value of the fuel increases. Generally, a fuel with a higher heating value tends to have lower HC emissions. However, in our case, when it comes to B80T20, a lower premixed combustion phase results in higher HC values compared to B80T20G75. This improves droplet evaporation of fuel, and subsequently, premixed combustion improves, resulting in increased combustion and a decrease in HC emissions. Lowest emission level was achieved for the GNP-enhanced fuels, with GNP50OCB20 recording the lowest value, at 52.2% and 50% relative to D100 and OCB20, respectively [46].

Overall, the B80T20G75 emits fewer hydrocarbons due to its superior premixed combustion over other GR dosages. The B80T20G75 resulted in a 25% lower HC level when compared with that of B80T20. The higher HC emission for the case of B80T20 (without GR) is due to poor combustion, a result also observed by other researchers for other NPs [54]. From the similar studies done by Bayindirli et al. [47] shown decrement of 15.73% for cottonseed oil methyl ester.

3.8 NO_x emissions

Figure 5e depicts the NO_x emission engine at various loads for B80T20 and various B80T20 -GR blends. The NO_x emission occurs during the premixed phase of the engine's fuel combustion. Premixed combustion is enhanced, and the combustion temperature increases as a result. Furthermore, the NOx content is low when the combustion temperature is low. However, as the load increases, fuel consumption also rises, resulting in higher NOx emission levels and higher combustion temperatures. Due to the presence of additional oxygen in its chemical composition, biodiesel has unique properties [55]. Furthermore, the increased availability of oxygen improved fuel combustion, resulting in a higher temperature within the chamber. The NO_x content increases with load in our studies, and this trend is also observed in the literature for other biodiesels [46]. However, increased NO_x content is observed in our studies due to the excess biodiesel (80%) as stated earlier. GR addition increases the NO_x levels as GR exhibits higher thermal conductivity and specific heat, which is responsible for improved pre-combustion and increased temperature, ultimately leading to higher NO_x emissions. The amount of NO_x due to the burning of fuel is associated with its heating value and the combustion process, where fuels with higher heating values (with increased GR) may result in increased NO_x emissions. However, the NO_x emission was found to decrease for a GR dosage of 100 mg/L. Due to increased biodiesel combustion, which raises NO_x emissions, B80T20G100 has lower NO_x emissions than B80T20G75, indicating that excess GR does not result in an increased NOx content beyond a certain level of GR dosage, likely due to agglomeration issues. B80T20G100 results in higher NO_x content at increased load conditions. For B80T20G75, the NO_x level increased by 8.16% compared to that of B80T20.

3.9 Smoke opacity

Another main pollutant from diesel engines is smoke. Figure 5f represents the result of graphene addition on smoke opacity according to load variations. The increase in engine load increases engine smoke opacity as fuel consumption increases. The GR dosage of 75 mg/L resulted decreased smoke opacity compared to other dosages. The addition of GR increases the surface-to-volume ratio, improving the evaporation of biodiesel spray droplets. Furthermore, GR, being in the liquid, enhances the dispersion and atomization of the droplets through breakup during injection. As a result, the fuel's ignition characteristics improve. Accelerated biodiesel oxidation and faster flame propagation reduce engine smoke [56]. The reduction in the smoke level of B80T20G75 is 10.16% as compared to B80T20.

The GR dosage of 75 mg/L results in a reduction in smoke, which is attributed to the large surface area of the GR, enhancing combustion by reducing the ignition delay and enabling complete fuel combustion, thereby lowering the smoke level as observed for other nano additives [57].

3.10 Regression analysis of BTE with respect to dosages and load conditions

Data matrix used for regression analysis resembles a design plan for a full factorial and without any replicates. However, we have a regression analysis based on RSM with uncoded units. Randomized data sets (Table 4) are provided in Fig. 6a, which includes residual analysis, detailing the occurrences. The significant and associated interactions of the load and dosage were assessed through statistical RSM analysis. Table 5 presents the results, including both main and interaction effects, the model coefficients, and the calculated standard deviations for all coefficients. The coded coefficients are also provided in Table 6. It is concluded from the table that the most influential variables are GR dosage and load. As shown in the figure, the BTE increases with load, and the addition of GR has a significant effect. The dosage has a positive influence on BTE up to 80%(Fig. 6c). The difference in BTE is observed during lower loads and the same is found to be small during higher loads, and the effect of dosage was found to be very significant for dosages more than 80%, as detailed below.

All above analysis have R2 fit as shown in Table 6.

Furthermore, a close observation of Fig. 6c reveals the BTE values for dosages of 0–50 and 60–100 mg/L for loads of 80–100%. In the former case, the difference is small. This leads to the conclusion that, up to 50 mg/L, the effect of GR on BTE is minimal, but there is an increasing trend up to a concentration of 75 mg/L. For the latter case, the

Table 4 Analysis of variance

Source	DF	Adj SS	Adj MS	F-Value	*P*-Value
Model	5	519.047	103.809	371.06	0.000
Linear	2	473.283	236.642	845.87	0.000
load	I	471.189	471.189	1684.25	0.000
dosage	1	2.095	2.095	7.49	0.021
Square	2	27.707	13.854	49.52	0.000
load*load	1	27.379	27.379	97.87	0.000
dosage*dosage	1	0.328	0.328	1.17	0.304
2-Way Interaction	1	0.297	0.297	1.06	0.327
load*dosage	1	0.297	0.297	1.06	0.327
Error	10	2.798	0.280		
Total	15	521.845			

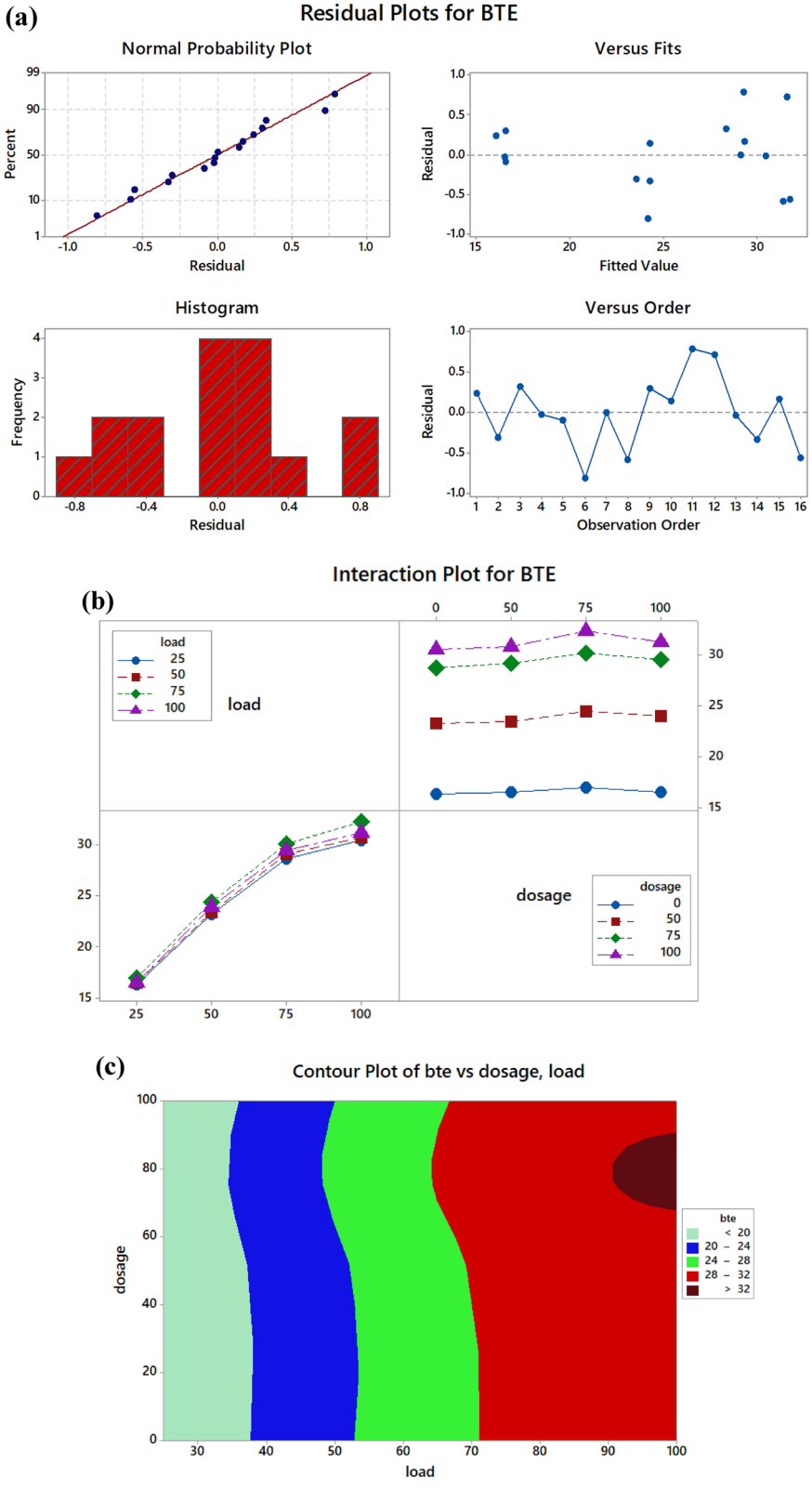

Fig. 6 **a**) Residual plots for CO **b**) Interaction plots among parameters involved in the emission of CO **c**) Contour plots of CO vs. dosage and load

Table 5 Coded coefficients

Term	Effect	Coef	SE Coef	T-Value	*P*-Value	VIF
Constant		27.002	0.28	96.27	0	
load	14.818	7.409	0.185	40.04	0	1.03
dosage	0.858	0.429	0.185	2.32	0.043	1.01
load*load	−6.036	−3.018	0.306	−9.86	0	1
dosage*dosage	−0.526	−0.263	0.307	−0.86	0.412	1.01
load*dosage	0.412	0.206	0.247	0.84	0.423	1.03

Table 6 R^2 values

	R-sq	*R*-sq(adj)	*R*-sq(pred)
BTE	99.44	99.15	98.64
CO	99.18	98.76	98.30
HC	95.05	92.57	89.96
NO_x	98.89%	98.33	97.41

BTE increased compared to the former case, but there was little variation after 80 mg/L. This indicates that the dosage does not result in any significant variation in BTE at a dosage value of 80 mg/L. This is due to the fact that increased GR content also leads to the problem of atomization. The higher GR dosage may cause agglomeration, resulting in inconsistent fuel quality that affects the effectiveness of GR in enhancing the combustion of the biodiesel blend. The optimum zones are those above 80 mg/L for loads of 80–90%, as seen in the plots in the top portion of the dark green bands. Interaction plots reveal there are interactions among parametric variations (Fig. 7). The generalized equation with uncoded units.

BTE = 5.923 + 0.4603 load + 0.0122 dosage − 0.002146 load*load − 0.000105 dosage*dosage + 0.000110 load*dosage.

3.11 Regression analysis of emission parameters with respect to dosages and load conditions

i) Regression analysis on emission components (CO) and corresponding residual plots and interaction plots are given in Fig. 8. Randomized data sets (Table 4), residual analysis is provided in Fig. 7a, comprising occurrences.

The randomized data sets for the analysis are given in Table 4. The residual analysis is provided in Fig. 8a, which includes occurrences of residuals, fitted values, and observation order. It is demonstrated through Fig. 8b that CO increases with load, and the addition of GR has a significant effect, leading to a reduction in CO values to a dosage value of 80 mg/L. The dosage has a positive influence on CO reduction up to 80 mg/L (Fig. 8c). It is observed that up to a 55% load, the CO values remain the same, i.e., 0.02 g/kWh. The CO variation during lower dosage remains sluggish for the lower load condition, with about 55% load, without much variation up to 60 mg/L. From Fig. 8c, it is also noted that the lower values of HC are observed for 75–85 mg/L. For dosages exceeding 80%, the HC reduction is of a diminishing nature.

Regression Equation in Uncoded Units.

CO = 0.04647 − 0.001851 Load − 0.000023 Dosage + 0.000025 Load*Load + 0.000001 Dosage*Dosage − 0.000002 Load*Dosage.

Table 7 Comparison of experimental values and RSM results

LOAD (%)	DOSAGE (GMS)	BTE (EXP)	BTE (RSM)	DIFF (%)	CO (EXP)	CO (RSM)	DIFF (%)	HC (EXP)	HC (RSM)	DIFF (%)	NO_X (EXP)	NO_X RSM	DIFF (%)
25	0	16.33	16.08967	1.471732	0.017	0.015828	6.894576	14	13.88006	0.119935	466	448.8278	3.685023
50	0	23.27	23.57399	1.306381	0.013	0.016435	26.42358	17	17.63578	0.635779	851	881.2335	3.552703
75	0	28.7	28.37582	1.129535	0.048	0.048292	0.608766	23	23.64149	0.641494	1320	1269.639	3.815211
100	0	30.48	30.49515	0.049711	0.112	0.111399	0.536294	32	31.89721	0.102792	1593	1614.045	1.321088
25	50	16.49	16.57532	0.517429	0.016	0.0136	14.99797	13	11.9089	1.091104	470	475.3475	1.137773
50	50	23.39	24.19714	3.450784	0.012	0.011579	3.509199	17	15.08175	1.918247	856	930.3704	8.68813
75	50	29.14	29.13645	0.012174	0.047	0.040807	13.1756	22	20.50461	1.49539	1378	1341.393	2.656513
100	50	30.81	31.39327	1.893109	0.104	0.101286	2.609578	30	28.17747	1.822532	1654	1708.416	3.28997
25	75	16.92	16.62094	1.767512	0.012	0.013663	13.85552	10	11.53695	1.536948	502	469.9938	6.375744
50	75	24.46	24.31149	0.607138	0.009	0.010327	14.74387	12	14.41838	2.418377	885	936.3252	5.799457
75	75	30.11	29.31955	2.625203	0.032	0.038241	19.50386	18	19.54981	1.549805	1456	1358.657	6.685671
100	75	32.37	31.64511	2.239393	0.091	0.097406	7.039032	24	26.93123	2.931234	1789	1736.988	2.90732
25	100	16.51	16.53507	0.151864	0.014	0.014509	3.636364	12	11.57409	0.425909	482	452.2309	6.17616
50	100	23.97	24.29437	1.353245	0.01	0.009859	1.409091	15	14.16409	0.835909	865	929.8709	7.499527
75	100	29.54	29.37117	0.571521	0.041	0.036459	11.07539	20	19.00409	0.995909	1400	1363.511	2.606364
100	100	31.21	31.76547	1.779791	0.096	0.094309	1.761364	27	26.09409	0.905909	1703	1753.151	2.944857
Error rate				1.307907			8.861253			1.214205			4.321344

- Regression analysis on emission components (HC) and corresponding interaction plots are given in Fig. 8.

The randomized data sets for the analysis are given in Table 4. The residual analysis is provided in Fig. 8a, which comprises occurrences of residuals. It is demonstrated through Fig. 8b that HC increases with load, and the addition of graphene has a significant effect, leading to a reduction in HC values to a dosage value of 80 mg/L. The dosage has a positive influence on HC reduction up to 80 mg/L (Fig. 8c). The in-HC values during lower dosage remain sluggish for lower load conditions, ranging from about 35–65% load. From Fig. 8c, it is also noted that the lower values of HC are observed for 75–85 mg/L. For dosages exceeding 80%, the HC reduction is of a diminishing nature.

Regression Equation in Uncoded Units.

HC = 12.37 + 0.0152 Load − 0.0441 Dosage + 0.001800 Load *Load + 0.000327 Dosage*Dosage − 0.000466 Load*Dosage.

iii) Regression analysis emission component NO_x and corresponding interaction plots are given in Fig. 9.

The randomized data sets for the analysis are given in Table 4. The residual analysis is provided in Fig. 9a, which includes occurrence residuals, fitted values, and observation order. It is observed in Fig. 9b that NOx increases with load, and the addition of GR has an adverse effect on the reduction of NOx emission; therefore, it is recommended to have a lower dosage. However, after 80 mg/L, the GR dosage has shown a positive influence (Fig. 9c). A difference in NOx values is observed at lower loads, and this effect is found to be sluggish at higher loads.

Regression Equation in Uncoded Units.

NO_x = 132.2 + 14.06 Load + 0.70 Dosage + 0.0101 Load*Load − 0.0080 Dosage*Dosage + 0.0140 Load*Dosage.

3.12 Multiple response regression analysis

To establish this, variables such as load and GR dosage are considered influencing factors, and responses including BTE, HC, CO, and NOx are examined. Two cases where the set parameters are shown in the overlaid contour plots (Fig. 10) below. For case 1 (Fig. 10a), the BTE value for the range of 30–35 is considered. For case 2(Fig. 10b), the BTE ranges from 25 to 35, and NO_x is restricted to 0–1000. For both cases, the feasible range of dosage and load values has been shown.

3.13 Economics related to the usage of nanoparticles

In this study, a preliminary cost analysis was conducted to assess the economic feasibility of incorporating GR as a fuel additive. The average diesel price in India is approximately ₹90 per litre, which corresponds to about US $1.02 per litre. The Commercial GR costs around US $0.00113 per mg, and based on the optimum dosage identified in this work, 75 mg/L, the additional cost of GR is approximately US $0.085 per liter. The engine tests revealed that adding GR increased BTE by 6.2%, resulting in reduced fuel consumption. This efficiency gain results in a fuel-saving value of roughly US $0.060 per litre. After accounting for these savings, the net additional cost attributed to GR is reduced to only US$0.025 per liter. Although a small net cost remains, the improved energy efficiency, enhanced combustion, and reduced emissions provide substantial operational and environmental benefits.

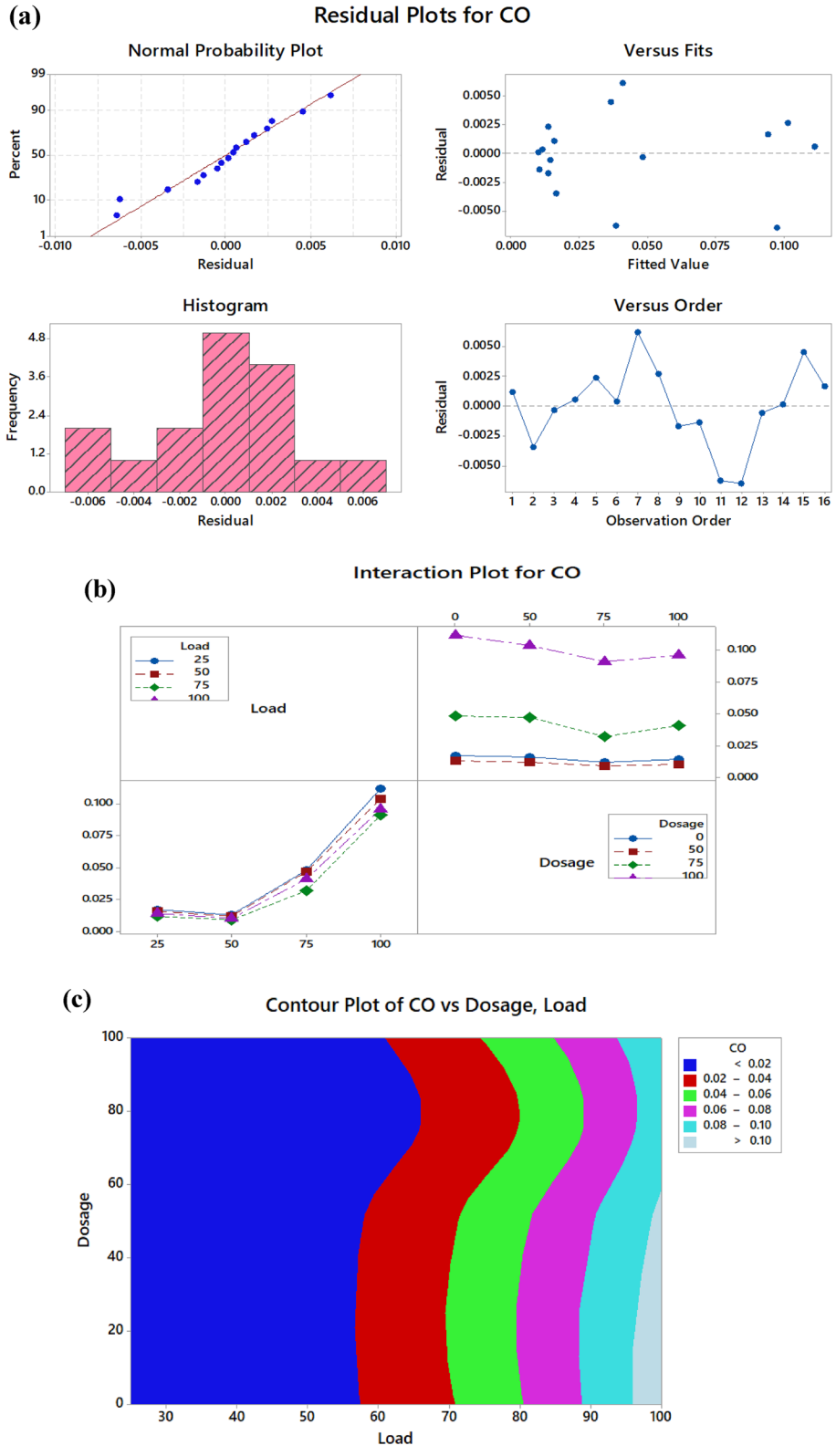

Fig. 7 **a**) Residual plots for CO **b**) Interaction plots among parameters involved in the emission of CO **c**) Contour plots of CO vs. dosage and load

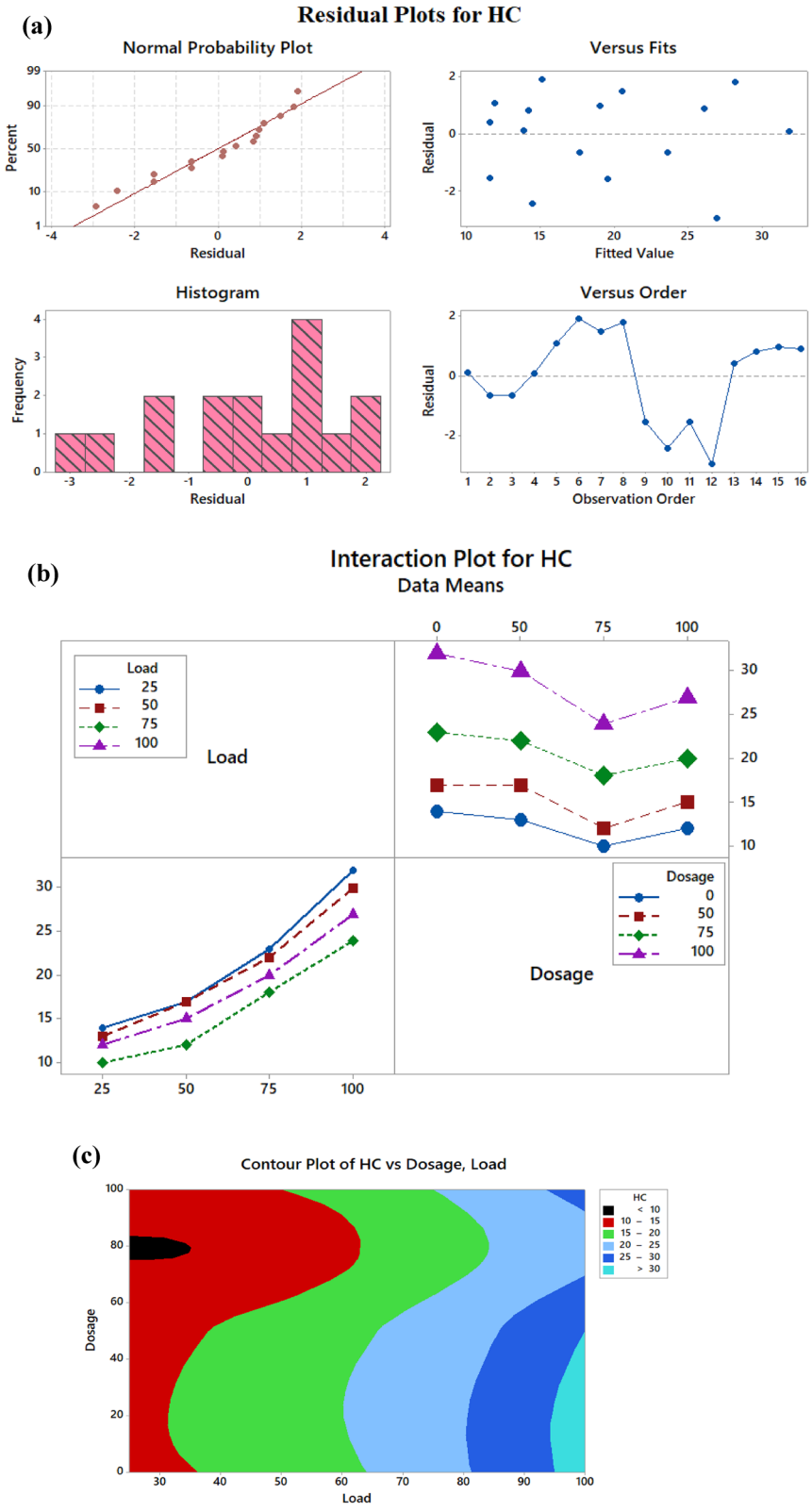

Fig. 8 **a**) Residual plots for HC **b**) Interaction plots among parameters involved in the emission of HC **c**) Contour plots of HC vs. dosage and load

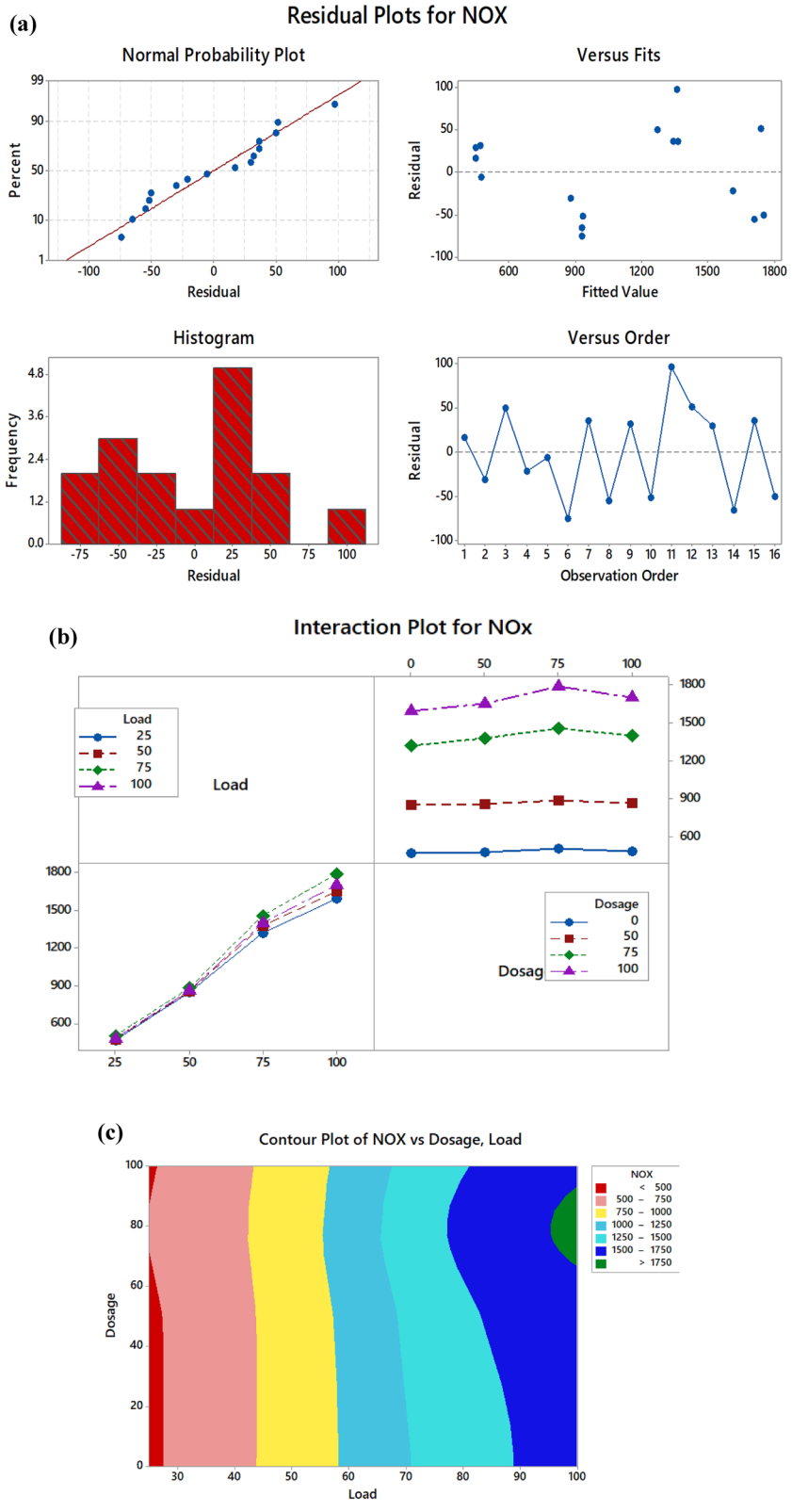

Fig. 9 **a**) Residual plots for NOx **b**) Interaction plots among parameters involved in the emission of NOx **c**) Contour plots of NO_x vs. dosage and load

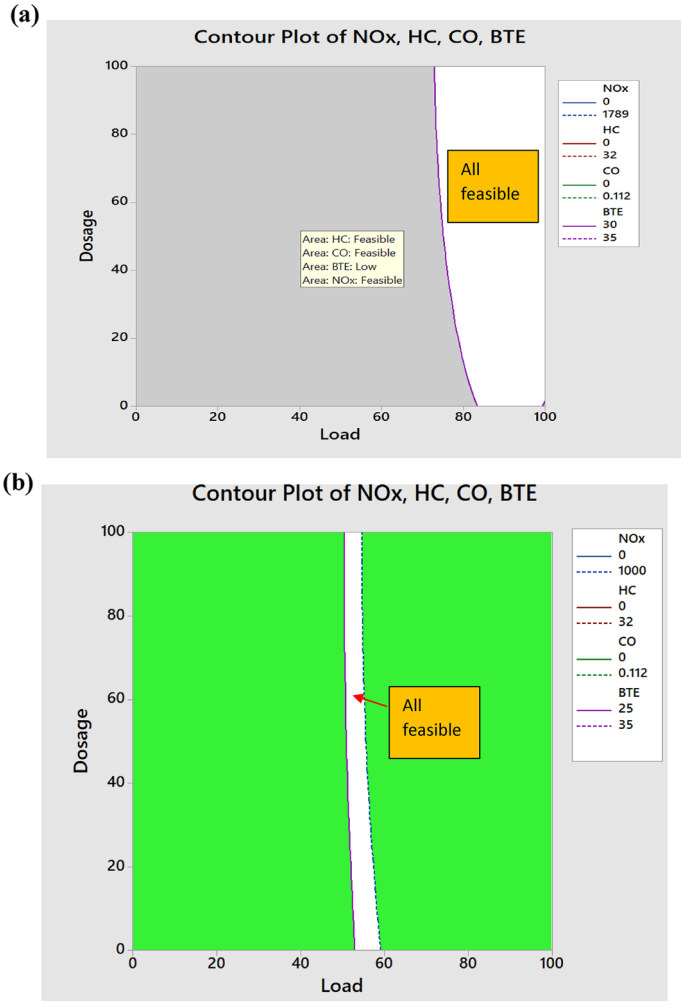

Fig. 10 Multiple response analysis for (**a**) case1, (**b**) case2

The study demonstrates that blending KOB with TPO in an 80:20 volume ratio effectively reduces the viscosity of the fuel and enhances its calorific value compared to pure biodiesel. Furthermore, the addition of GR to this blended fuel significantly improves the engine's brake thermal efficiency and contributes to a noticeable reduction in exhaust emissions, including CO and smoke opacity. These improvements suggest that the KOB–TPO–GR combination presents a promising alternative fuel formulation, offering enhanced combustion and emission characteristics compared to conventional biodiesel blends.

4 Main findings

The study demonstrates that blending KOB with TPO in an 80:20 volume ratio effectively reduces the viscosity of the fuel and enhances its calorific value compared to base fuel mixture. Furthermore, the addition of GR to this blended fuel significantly improves the engine's BTE. It contributes to a noticeable reduction in exhaust emissions, including CO and smoke opacity. These improvements suggest that the KOB–TPO–GR combination presents a promising alternative fuel formulation, offering enhanced combustion and emission characteristics compared to conventional biodiesel blends.

5 Limitations

The present study is limited by the specific fuel blend ratio and GR dosages considered. Only a single blend ratio of 80% KOB and 20% TPO was investigated on a volume basis, which may not fully capture the influence of varying blend proportions on engine performance and emissions. Similarly, the GR dosage was restricted to three dosage levels, which limits the ability to identify the absolute optimum dosage or to establish a more detailed trend of its effects. Future studies should explore a wider range of KOB–TPO blend ratios and GR dosages, along with potential interactions between fuel composition and nanoparticle loading, to develop a more comprehensive understanding of their combined influence on combustion behavior, performance, and emission characteristics.

6 Scope for future work

The findings of this study highlight the potential of KOB–TPO–GR blends as a cleaner and more efficient alternative to conventional biodiesel. Future research should focus on exploring a wider range of blend ratios and nanoparticle concentrations to identify the optimal combination for various engine types and operating conditions. Detailed investigations into combustion kinetics, long-term engine durability, and GR dispersion stability would further enhance understanding of the underlying mechanisms. Additionally, life-cycle assessment and techno-economic analysis could provide insights into the large-scale feasibility and environmental impact of implementing such nanofuel blends in practical applications.

7 Conclusion

One method of reducing the viscosity of biodiesel is to blend it with another fuel that has a lower viscosity and a higher calorific value. Hence, in this work, TPO was added to biodiesel. An investigation of the blending of TPO with KOB and GR has been undertaken. The standard FTIR technique was used to confirm the mixing properties of TPO-blended KOB combined with GR. The findings from these analyses were encouraging, enabling the incorporation of TPO and GR, prompting the authors to explore the thermal performance. The variation in BTE and emissions was observed as the dosage of nanoparticles increased from 0 to 100 mg/L. However, it was observed that there is a limiting dosage value beyond which the trend varies.

The increment in BTE is observed with an increase in the dosage of GR. But the B80T20G75 demonstrates a 6.2% increase in BTE compared to the B80T20 at full load. From the optimization plots, it is observed that the ideal zones are those exceeding 80 g for loads ranging from 80% to 90%. An increase in GR dosage influences the spray characteristics of the fuel mixture, which impacts combustion pressure and subsequently lowers the engine's BTE. When comparing B80T20G75 to B80T20, the CO emissions are decreased by 18.75%. The B80T20G75 also shows a 25% reduction in HC levels compared to B80T20. Regarding NO_x emissions, B80T20G75 indicates a 12.3% rise relative to B80T20.

Additionally, the NO_x levels for B80T20G75 have increased by 12.3% compared to B80T20. The improvements in thermal efficiency and the reductions in engine emissions were quantified in terms of percentage and. revealed a significant improvement in BTE, along with a noticeable reduction in CO, HC and smoke opacity. They were found to be

substantially higher than the estimated experimental error margins, thereby confirming the effectiveness of the tested system and the validity of the results.

In summary, additives like GR in a moderate dosage of 50 gms to 75 gms to B80T20 improve the engine BTE, and it dramatically lowers particle, HC, and CO_2 emissions from engines. However, it causes higher NO_x contents due to increased heat release and a higher rate of combustion. The regression analysis helps to obtain the required correlation for various responses among dependent variables. The results indicate that GR can be a better alternative to other nanoparticles, such as Al_2O_3 and TiO_2, for reducing emissions. Based on the beneficial effects of adding TPO along with nanoparticles, the study can be further extended to other types of biodiesels, taking TPO as a secondary blend. The best biodiesel/nanoparticle combination can be proposed considering both performance and emission characteristics.

The study demonstrates that blending KOB with TPO in an 80:20 volume ratio effectively reduces the viscosity of the fuel and enhances its calorific value compared to pure biodiesel. Furthermore, the addition of GR to this blended fuel significantly improves the engine's BTE and contributes to a noticeable reduction in exhaust emissions, including CO and smoke opacity. These improvements suggest that the KOB–TPO–GR combination presents a promising alternative fuel formulation, offering enhanced combustion and emission characteristics compared to conventional biodiesel blends.

Abbreviations

ASTM	American Society of Testing of Materials
BTE	Brake Thermal Efficiency
CO	Carbon Monoxide
CPO	Crude Palm Oil
EGR	Exhaust Gas Recirculation
GR	Graphene
FAME	Fatty Acid Methyl Ester
FTIR	Fourier transform infrared Spectroscopy
GNP	Graphene Nanoparticles
GR	Graphene
HC	Hydrocarbons
HVO	Hydrotreated Vegetable Oil
KO	Karanja Oil
NO	Nitric oxide
NOx	Oxides of nitrogen
OD	Ordinary Diesel
OCB	Oleander and Croton Biodiesel
KOB	Karanja Oil Biodiesel
PAH	Polycyclic aromatic hydrocarbons
TPO	Tyre Pyrolysis Oil
B80T20(80% KOB+20%TPO) B80T20G50, B80T20G75 and B80T20G100	-B80T20+50 mg/L GR, B80T20+75 mg/L GR and B80T20+100 mg/LGR
PBD20	-(10%pyrolysis oil + 10%biodiesel + 80% diesel
OCB2	Oleander and Croton Biodiesel
NP	Nanoparticles

Acknowledgements
The authors acknowledge Nitte Meenakshi Institute of Technology and Manipal Academy of Higher Education for their support in writing this paper.

Author contributions
Conceptualization–Dr. Kapilan Natesan; Methodology– Sadashiva Prabhu S; Investigation– Dr. Kapilan Natesan; Resources– Dr. Kapilan Natesan; Data curation– Sadashiva Prabhu S, Dr.Norkhairunnisa Mazlan; Writing and original draft

preparation– Dr. Sadashiva Prabhu S; Writing, review and editing- Dr. Shivaprakash YM; visualization– Dr. Gurumurthy BM, Dr.Norkhairunnisa Mazlan; supervision– Dr. Kapilan Natesan. All authors confirm their shared responsibility and commitment to be accountable for all aspects of this research work.

Funding
Open access funding provided by Manipal Academy of Higher Education, Manipal. The authors receive no funding for this work.

Data Availability
The datasets generated during and/or analysed during the current study are available from the corresponding author on reasonable request.

Code Availability
Not Applicable.

Declarations

Ethics approval and consent to participate
Not applicable.

Consent for publications
Not applicable.

Competing interests
The authors declare no competing interests.

Received: 13 October 2025 / Accepted: 24 December 2025
Published online: 15 January 2026

References

1. Knothe G, Razon LF. Biodiesel fuels. Prog Energy Combust Sci. 2017;58:36–59.
2. Lai JYW, Lin KC, Violi A. Biodiesel combustion: advances in chemical kinetic modeling. Prog Energy Combust Sci. 2011;37:1–14.
3. K.Dhanasekar M, Sridaran M, Arivanandhan RJ. A facile preparation, performance and emission analysis of *Pongamia* oil based novel biodiesel in diesel engine with CeO2:Gd nanoparticles. Fuel. 2019;255:Article ID:115756.
4. Rowe BYD. Beyond food versus fuel S6 Nature 2008;474:3–5.
5. Gebremariam Shemelis Nigatu. Biodiesel as a transport fuel, advantages and disadvantages: review. Biofuels Bioprod Biorefin. 2023;17(5):1115–477.
6. Malik MAI, Zeeshan S, Khubaib M, Ikram A, Hussain F, Yassin H. Atika Qazi, a review of major trends, opportunities, and technical challenges in biodiesel production from waste sources, energy conversion and management. 2024;X 23:Article ID:100675. https://doi.org/10.1016/j.ecmx.2024.100675.
7. Rohtagi PK. Biodiesel in India—a review. Advances in Fluid and Thermal Engineering: Select Proceedings of FLAME 2020. 2021;741–51.
8. Dong VH, Le QT. Physical properties and spray characteristics of ultrasound-assisted emulsion based on ultra-low sulphur diesel and biodiesel. Int J Technol. 2019;10(2):247–57.
9. Silva NDLD, Batistella CB, Filho RM, Maciel MRW. Biodiesel production from castor oil: optimization of alkaline ethanolysis. Energy Fuels. 2009;23(11):5636–42.
10. I.B.B.Ilić OS. Biodiesel production from non-edible plant oils. Renew Sustain Energy Rev. 2012;16(6):3621–47.
11. Hoseini SS, Najafi G, Ghobadian B, Mamat R, Ebadi MT, Yusaf T. Novel environmentally friendly fuel: the effects of nanographene oxide additives on the performance and emission characteristics of diesel engines fuelled with *Ailanthus altissima* biodiesel. Renew Energy. 2018;125:283–94.
12. Senthil R, Silambarasan R, Munusami V, Veerappan D. Effect of antioxidant additives on oxides of nitrogen (NO_x) emission reduction from Annona biodiesel operated diesel engine. Renew Energy. 2020;148:1321–6.
13. Sharma N, Bachalo W.D., Agarwal A.K. Spray droplet size distribution and droplet velocity measurements in a firing optical engine. Phys Fluids. 2020;32(2):ArticleID:023304.
14. Dhar A. Experimental investigations of the effect of pilot injection on performance, emissions and combustion characteristics of *Karanja* biodiesel fuelled CRDI engine. Energy Convers Manage. 2015;93:357–66.
15. Shahabuddin M, Liaquat AM, Masjuki HH, Kalam MA, Mofijur M. Ignition delay, combustion and emission characteristics of diesel engine fuelled with biodiesel. Renew Sustain Energy Rev. 2013;21:623–32.
16. Kalam MA, Masjuki HH. Emissions and deposit characteristics of a small diesel engine when operated on preheated crude palm oil. Biomass Bioenergy. 2004;27(3):289–97.
17. Changmai B, Vanlalveni C, Prabhakar Ingle A, Bhagat R, Lalthazuala Rokhum S. Widely used catalysts in biodiesel production: a review. RSC Adv. 2020:10:41625–79.
18. Harreh D, Saleh AA, Reddy ANR, Hamdan S. An experimental investigation of Karanja biodiesel production in Sarawak, Malaysia. J Eng. 2018; Article ID: 4174205.
19. Patel C, Chandra K, Hwang J, Agarwal RA, Gupta N, Bae C. Comparative compression ignition engine performance, combustion, and emission characteristics, and trace metals in particulates from waste cooking oil, *Jatropha* and *Karanja* oil derived biodiesels. Fuel. 2019;236:1366–76.
20. Gowthaman S,and Thangavel K, Performance, emission and combustion characteristics of a diesel engine fuelled with diesel/coconut shell oil blends. Fuel 2022;322:Article ID:124293.

21. Mohite S, Kumar S, Maji S. Performance characteristics of mix oil biodiesel blends with smoke emissions. International Journal of Renewable Energy Development. 2016;5(2):163–70.
22. Sudalaiyandi K, Karthick Alagar V, Kumar R, Manoj Praveen VJ, Madhu P. Performance and emission characteristics of a diesel engine fueled with ternary blends of linseed and rubber seed oil biodiesel. Fuel. 2021;285:Article ID:119255.
23. Vihar R, Baškovič UŽ, Seljak T, Katrašnik T. Combustion and emission formation phenomena of tire pyrolysis oil in a common rail Diesel engine. Energy Convers Manag. 2017;149:706–21.
24. Murugan S, Ramaswamy MC. The use of tyre pyrolysis oil in diesel engines. Waste Manag. 2008;28:2743–9.
25. Auti SM, Rathod WS. Effect of hybrid blends of raw tyre pyrolysis oil, karanja biodiesel and diesel fuel on single cylinder four stokes diesel engine. Energy Rep. 2021;7:2214–20. https://doi.org/10.1016/j.egyr.2021.04.007.
26. Saravanakumar K, Robinson Y, Sowmya Dhanalakshmi C, Madhu P. Improving the poor properties of Methyl ester with pyrolysis oil and fossil diesel – An experimental investigation on PSZ ceramic coated engine with the addition of GO nanoparticles. Indian J Chem Technol. 2024;21(4):553–63.
27. Rajak U, Nashine P, Chaurasiya PK, et al. The effects on performance and emission characteristics of DI engine fuelled with CeO2 nanoparticles addition in diesel/tyre pyrolysis oil blends. Environ Dev Sustain. 2025;27:22635–62. https://doi.org/10.1007/s10668-022-02358-8.
28. Kapilan N, K Ganesh., S Balaji. Experimental investigation on effect of nano particles on performance and emission characteristics of diesel engine fuelled with waste cooking oil biodiesel. J Mines Met Fuels. 2022;70(10A):297–301.
29. Ahmed MM, Pali HS, Khan MM. Feasibility of nanoparticles fused in biodiesel for CI engines: an integrated and historic review. J Therm Anal Calorim. 2024;149:5091–123.
30. Bahaaddein KM, Mahgoub. Effect of nano-biodiesel blends on CI engine performance, emissions and combustion characteristics –. Rev Heliyon. 2023;9(11):e21367.
31. Bitire SO, Nwanna EC, Jen T-C. The impact of CuO nanoparticles as fuel additives in biodiesel-blend fuelled diesel engine: a review. Energy Environ. 2023;34(7):2259–89.
32. Sekhar PC, Kumara Swami Gupta AVSS. Diesel-biodiesel blends using nanoparticles with dispersants: combustion, performance, and emissions analysis. Next Mater. 2025;9:101146.
33. Dhairiyasamy R, Dixit S, Singh S, Gabiriel D. A comprehensive analysis of combustion efficiency and emissions in biodiesel blends for sustainable energy solutions. Int J Thermofluids. 2025;29:101357. https://doi.org/10.1016/j.ijft.2025.101357.
34. Çelik Mehmet. An experimental investigation on improving combustion characteristics and environmental effects of biodiesel-diesel blend with multi-walled carbon nanotubes. Fuel. 2026;407:137257. https://doi.org/10.1016/j.fuel.2025.137257.
35. Barai DP, Bhanvase BA, Sonawane SH. A review on graphene derivatives-based nanofluids: investigation on properties and heat transfer characteristics. Ind Eng Chem Res. 2020;59:10231–77.
36. El-Seesy AI, Hassan H, Ookawara S. Effects of graphene nanoplatelet addition to jatropha biodiesel–diesel mixture on the performance and emission characteristics of a diesel engine. Energy. 2018;147:1129–52.
37. Sharma V, Hossain AK, Ahmed A. A.Rez, Study on using graphene and graphite nanoparticles as fuel additives in waste cooking oil biodiesel. Fuel. 2022;328:Article ID:125270.
38. Uysal C, Ağbulut Ü, Elibol E, Demirci T, Karagoz M, Saridemir S. Exergetic, exergoeconomic, and sustainability analyses of diesel–biodiesel fuel blends including synthesized graphene oxide nanoparticles. Fuel. 2022;327(3):Article ID:125167.
39. Stephen Livingston T, Madhu P, Sowmya Dhanalakshmi C, Vignesh Kumar R. An experimental investigation on performance, emission and combustion characteristics of IC engine using liquid fuel produced through catalytic co-pyrolysis of pressed oil cake and mixed plastics with the addition of nanoparticles. Fuel. 2025;379:Article ID:133092.
40. Josephin J S Femilda, Subramanian Balaji, Jeslin Renjit E, Venkatesh S Naveen, Sugumaran V, Subramanian Thiyagarajan, et al. Tree-based ensemble regression models for emission prediction of a winter green oil-hydrogen dual-fuel engine with zeolite after-treatment. Renew Energy. 2026;257:124726. https://doi.org/10.1016/j.renene.2025.124726.
41. Akbari M, Piri H, Renzi M, Bietresato M. The effects of biodiesel on the performance and gas emissions of farm tractors' engines: a systematic review, meta-analysis, and meta-regression. Energies. 2024;17(17):4226. https://doi.org/10.3390/en17174226.
42. Sadashiva Prabhu S, Natesan Kapilan, Shivaprakash YM, Gurumurthy BM. Mixing, burning and deposit characteristics of a mixture of karanja oil biodiesel and tyre pyrolysis oil along with graphene nanoparticles. Int Rev Mech Eng. 2024;18(6):295–303. https://doi.org/10.15866/ireme.v18i6.24576.
43. Man XJ, Cheung CS, Ning Z, Wei L, Huang ZH. Influence of engine load and speed on regulated and unregulated emissions of a diesel engine fuelled with diesel fuel blended with waste cooking oil biodiesel. Fuel. 2016;180:41–9.
44. Daho T, Vaitilingom G, Ouiminga SK, Piriou B, Zongo AS, Ouoba S. Influence of engine load and fuel droplet size on performance of a CI engine fuelled with cottonseed oil and its blends with diesel fuel. Appl Energy. 2013;111:1046–53.
45. M.Norhafana MM. A review of the performance and emissions of nano additives in diesel fuelled compression ignition-engines, 1st International Postgraduate Conference on Mechanical Engineering (IPCME2018) 31 October 2018, UMP Pekan, Pahang, Malaysia, IOP Conference Series: Materials Science and Engineering 2019;469: 012035.
46. Wambui T, Hawi M, Njoka F, Kamau J. Performance enhancement and emissions reduction in a diesel engine using oleander and croton biodiesel doped with graphene nanoparticles. Int J Renew Energy Dev. 2023;12(3):635–47.
47. Cihan Bayindirli M, Celik Recep Zan,Optimizing the thermophysical properties and combustion performance of biodiesel by graphite and reduced graphene oxide nanoparticle fuel additive,Engineering. Sci Technol Int J Volume. 2023;37. https://doi.org/10.1016/j.jestch.2022.101295.
48. Das Akkur Neele Gowda M, Riyazuddin HM, Nagaraj S, et al. Outcome of novel combination of graphene nanoparticles and Moringa methyl ester fueled engine working under varying loads and compression ratios. J Eng Appl Sci. 2024. https://doi.org/10.1186/s44147-024-00498-4.
49. Demir U, Çelebi S, Ozer ¨S. Experimental investigation of the effect of fuel oil,graphene and HHO gas addition to diesel fuel on engine performance and exhaust emissions in a diesel engine. Int J Hydrogen Energy. 2024;52:1434–46. https://doi.org/10.1016/j.ijhydene.2023.08.007.
50. Simsek S, Uslu S, Simsek H. Response surface methodology-based parameteroptimization of single-cylinder diesel engine fueled with graphene oxide dosed sesame oil/diesel fuel blend. Energy AI. 2022;10:Article ID:100200. https://doi.org/10.1016/j.egyai.2022.100200.

51. Basha JS, Anand RB. An experimental investigation in a diesel engine using carbon nanotubes blended water–diesel emulsion fuel. Proceedings of the Institution of Mechanical Engineers, Part A: Journal of Power and Energy. 2011;255(3):279–88.
52. Bidir MG, Narayanan Kalamegam M, Adaramola MS, Hagos FY, Chandra Singh R. Investigation of combustion, performance, and emissions of biodiesel blends using graphene nanoparticles as an additive. International Journal of Engine Research. 2022;24(11):4459–69.
53. Yadav M, Karimi MN, Yadav AK. Effect of graphene oxide nanoparticles dispersed biodiesel on combustion, performance and emission characteristics of a diesel engine. Proc Institution Mech Eng Part E: J Process Mech Eng. 2023;239(5):2612–24. https://doi.org/10.1177/09544089231209139.
54. Hosseini SH, Alisaraei AT, Ghobadian B, Mayvan AA. Effect of added alumina as nano-catalyst to diesel-biodiesel blends on performance and emission characteristics of CI engine. Energy. 2017;124:543–52.
55. Pham PX. Influences of Molecular Profiles of Biodiesels on Atomization, Combustion and Emission Characteristics. PhD. thesis. University of Sydney (2015).
56. Uyumaz A, Aydoğan B, Yilmaz E, Solmaz H, Aksoy F. I.Mutlu, Experimental investigation on the combustion, performance and exhaust emission characteristics of poppy oil biodiesel-diesel dual fuel combustion in a CI engine Fuel,2020;280, Article ID:118588.
57. Gad MS. S.Jayaraj, A comparative study on the effect of nano-additives on the performance and emissions of a diesel engine run on Jatropha biodiesel, fuel,2020; 267: Article ID:117168.

Publisher's note